



ELSEVIER

journal homepage: www.elsevier.com/locate/jmatprotec

Mott–Schottky analysis of aluminium oxide formed in the presence of different mediators on the surface of aluminium alloy 2024-T3

Kirill L. Levine^{a,*}, Dennis E. Tallman^{a,b}, Gordon P. Bierwagen^b

^a Department of Chemistry and Molecular Biology, North Dakota State University, Fargo, ND 58105-5516, United States

^b Department of Coatings and Polymeric Materials, North Dakota State University, Fargo, ND 58105-5516, United States

ARTICLE INFO

Article history:

Received 6 November 2006

Received in revised form

3 August 2007

Accepted 8 August 2007

Keywords:

Anodization

Electron transfer mediation

Mott–Schottky analysis

Aluminium alloys

Corrosion protection

ABSTRACT

Corrosion protection of aluminium (Al) alloys is an important industrial problem. In the past it was solved with hexavalent chromium (Cr⁶⁺) coatings. However, these coatings are hazardous, and have to be replaced. One of the most promising alternatives to Cr⁶⁺ corrosion protection technology is the protection with intrinsically conducting polymers (ICPs). In order to advance this type of protection, this is necessary to understand properties of Al oxide formed in the presence of the electron transfer mediators, compounds that allow ICPs deposition on Al alloy surface. Due to low thicknesses of oxide layers on Al (of the order of a few nanometers) only a limited number of methods can be used to study its properties. In this paper we report the research of the properties of Al oxide by Mott–Schottky analysis, electrochemical technique that allows determining a variety of oxide parameters treating it as a semiconductor, ultra-thin layer with non-stoichiometric defects or substitutions. Electrochemically determined flat band potential and concentration of charge carriers in the oxide are discussed in correlation with the structure of electron transfer mediator that was applied during the oxide formation.

© 2007 Elsevier B.V. All rights reserved.

1. Introduction

Aluminium (Al) alloy 2024-T3 is an important construction material due to its low weight and excellent mechanical properties. Chemically pure Al is naturally protected from corrosion by uniform oxide layer. However, Al alloys, such as Al 2024-T3, contain considerable percentage of impurities (Cu 3.8–4.9%, Mg 1.2–1.8%, Si 0.5%, Mn, Cr, Zn, Ti, Fe and other unspecified impurities 0.8–1.4%). These impurities form density fluctuations and alloy becomes vulnerable to galvanic corrosion. Annual losses due to corrosion encounter 1.5–2% of total Al constructions, requiring billions of dollars in maintenance and replacement (Koch, 2002). Until

today, corrosion protection of Al alloys was performed by hexavalent chromium (Cr⁶⁺) conversion coatings. However, technologies utilizing Cr⁶⁺ are considered by the Occupational Safety and Health Agency (OSHA) to be an environmental and health hazard, and have to be replaced. The most feasible approach to Cr⁶⁺ technology is intrinsically conducting polymer (ICP) technology (Iroh, 2001). ICPs can be deposited onto electrically conducting surface electrochemically; however depositing ICPs onto coated with an oxide layer surface is a challenge. Recently suggested approach to solve this problem utilizes so-called electron transfer mediators (ETMs), compounds that allow to decrease ICPs deposition potential (Tallman et al., 2002). ICPs performance is greatly affected

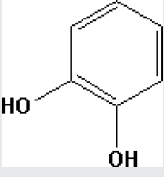
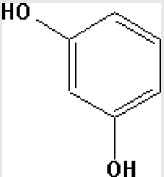
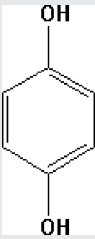
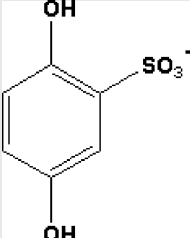
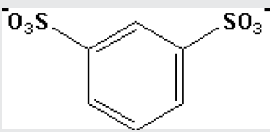
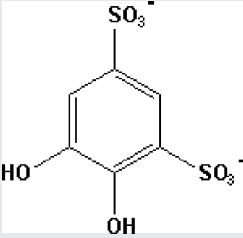
* Corresponding author. Current address: Department of Technology and Materials Research, State Polytechnical University of St. Petersburg, Polytechnicheskaya str. 29, Saint Petersburg 195251, Russia.

E-mail address: levinkl@hotmail.com (K.L. Levine).

0924-0136/\$ – see front matter © 2007 Elsevier B.V. All rights reserved.

doi:10.1016/j.jmatprotec.2007.08.023

Table 1 – Structures and abbreviated names of investigated compounds

Structure		Abbreviated name
	1,2-Dihydroxybenzene (catechol)	CAT
	1,3-Dihydroxybenzene (resorcinol)	RES
	1,4-Dihydroxybenzene (hydroquinone)	HQ
	Hydroquinone sulfonate	HQS
	Benzene disulfonate	BDS
	Dihydroxybenzene disulfonate	DHBDS

by Al oxide layer (Levine et al., 2005a) and understanding properties of oxide formed in ETM presence is necessary for successful ICPs deposition. The ETM influence of PPy deposition on Al alloy surface was described by Levine et al. (2005b). The ETM influence on Al oxide formation is reported in current paper. Studied compounds were benzenes with either hydroxyl, or sulfonate substitutions, or combination of both. Their structure is shown in Table 1. 1,2-Dihydroxybenzene (catechol (CAT)), 1,4-dihydroxybenzene (hydroquinone (HQ)), 1,3-dihydroxybenzene (resorcinol (RES)), benzene disulfonate (BDS), hydroquinone sulfonate (HQS), and 1,2-dihydroxybenzene, 3,4-disulfonate (DHBDS), also known as Tiron. Some of them (HQ and CAT) can be polymerized electrochemically on

an inert metallic surface; the others do not show this property. All compounds shown in Table 1 are soluble in water and demonstrate different performance as ETMs, ranging from the absence of mediation properties (RES) to high-mediation performance (DHBDS). In substituted benzenes, hydroxyl groups are responsible for the electron exchange between the monomer and the mediator, while sulfonate groups facilitate monomer penetration into Al oxide pores (Naoi et al., 2000). In the case where combination of both sulfonate and hydroxyl substitutions is within the same mediator, both of the above mechanisms act simultaneously.

The ETM structure affects properties of the electrical contact between ICP and Al alloy surface (Levine et al., 2005a),

therefore knowledge of Al oxide properties is of importance for further understanding the mechanism of mediation. Electrochemical impedance spectroscopy (EIS) is a versatile tool to study interfaces, allowing extraction variety of important coatings parameters (Mathias and Haas, 1992; Tolstopyatova et al., 2005). Studies of Al oxide by electrochemical method: Mott-Schottky (MS) analysis, are reported in this paper.

2. Experimental

2.1. Chemicals

DHBDS and CAT were obtained from Aldrich Chemical Company; sodium sulfate, HQ, HQS and BDS were obtained from Alfa Aesar. Technical grade HQS was purified by recrystallization. All other chemicals used were analytical grade. Al 2024-T3 panels were purchased from Q-Panel Co. and were prepared for electrodeposition by dry-polishing to 1500 grit with emery paper followed by rinsing with hexane. Solutions were prepared using Milli-Q water.

2.2. Methods

2.2.1. Cyclic voltammetry

Cyclic voltammetry (CV) was carried out using a BAS-100B Electrochemical Workstation manufactured by Bioanalytical Systems Inc. The one-compartment electrochemical cell consisted of a glass cylinder attached to a sample by metal clip with O-shaped rubber gasket. Sample was used as the working electrode, silver/silver chloride (Ag/AgCl) was used as the reference electrode, platinized grid was used as the counter electrode. The solution was composed of 1 M of sodium sulfate (Na_2SO_4) with or without of 0.1 M of a studied compound.

2.2.2. Mott-Schottky analysis and electrochemical impedance spectroscopy

MS analysis was performed by ESA 400 potentiostat manufactured by Gamry Electrochemical Instruments. Gamry Applied Research software was used for data acquisition. The same software package and cell assembly was used for EIS analysis. MS analysis was performed on CV prepared samples without removing sample from the electrochemical cell. Measurements were performed in 1 M Na_2SO_4 solution. Samples were equilibrated at an open-circuit potential (OCP) for 100 s before each experiment. Each measurement was repeated three times. The accuracy of data acquisition was 10% or better.

3. Results and discussion

3.1. Cyclic voltammetry

To increase the thickness of the oxide layer, samples were anodized by CV at a scan rate of 5 mV/s in the potential range from negative 1 V to positive E_{max} , similar as Levine et al. (2005b) (Fig. 1). Both in the presence and the absence of ETM, CV-gram revealed the shape typical for the process of oxide growth by high-field mechanism (Lorenge, 1993). Current during the first CV sweep (labeled “1” in Fig. 1) (in the positive direction) was by approximately two orders of magnitude higher than the current during sweep in the negative direction (labeled “2” in Fig. 1) due to the increased Ohmic resistance of formed oxide. Low currents were observed at a sweep numbers larger than one. They were almost superim-

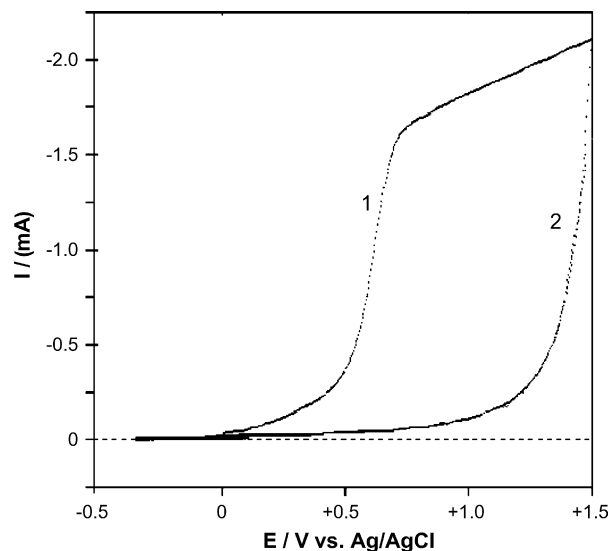


Fig. 1 – Cyclic voltammetry of Al2024-T3, five cycles. Scan rate 5 mV/s [Na_2SO_4 1 M].

posed with the curve “2” (Fig. 1) both in positive and negative directions, proving that the oxide layer was not dissolving during scanning in the negative direction.

3.2. Electrochemical impedance spectroscopy

EIS pattern of bare Al alloy surface shows a semicircular trace due to an oxide layer, possessing good barrier properties (Fig. 2, gray curve).

After CV scan the pattern changes to a semicircle with a larger radius, due to the increased impedance of the oxide (Fig. 2, black curve). Observed behavior can be visualized by Randles circuit (Fig. 3(A)), where R_s denotes the solution resistance, C_{ox} is the oxide capacitance and R_{ox} is the oxide resistance. Paying more attention to the physics, approxima-

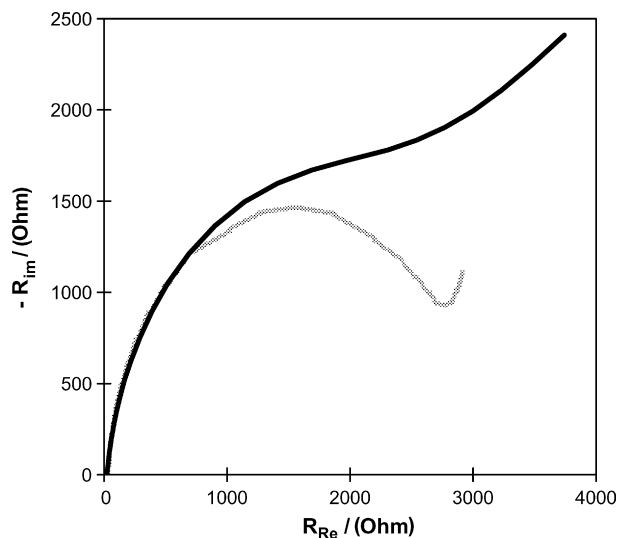


Fig. 2 – EIS of bare Al 2024-T3 surface (gray curve), and after CV (black curve) [Na_2SO_4 1 M], $E_{\text{max}} = 0.6$ V vs. Ag/AgCl, scan rate 5 mV/s, one cycle.

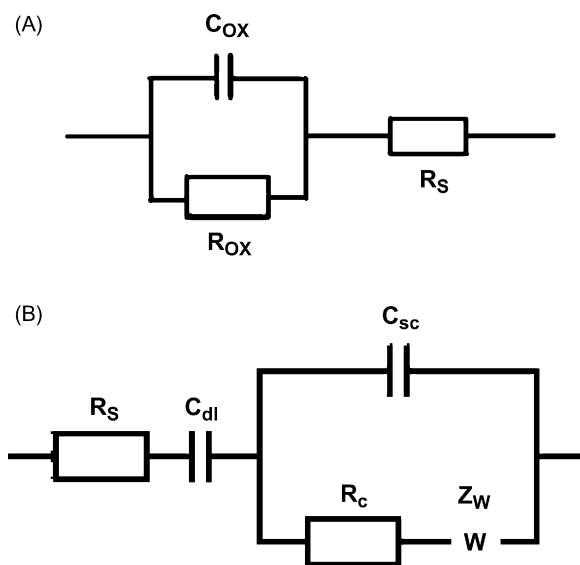


Fig. 3 – Equivalent circuit modeling of the electrochemical cell: (A) simplified circuit and (B) detailed circuit.

tion can be performed with the help of more complicated schematic shown in Fig. 3(B) (Simons et al., 1999; Bondarenko and Ragoisha, 2005), where C_{dl} is the product of the double electric layer (DEL) capacitance and Helmholtz capacitance, space charge capacitance, C_{sc} the overall electrode capacitance that in our case is mainly due to the oxide, R_c the charge transfer resistance and Z_w is the Warburg element describing frequency-dependent diffusion related resistance. Despite its simplicity, the scheme shown in Fig. 3(A) provides high (95%) fitting accuracy.¹

4. Mott-Schottky analysis

MS experiments were performed to characterize an oxide layer formed at the surface of Al alloy in the presence of different mediators.

The MS plot was constructed of the inverse square of space charge layer capacitance C_{sc}^{-2} measured at a fixed frequency of 1000 Hz as a function of potential around open-circuit potential (OCP) (Mott, 1939; Schottky, 1939) (Fig. 4). MS relationship for p type semiconductor can be written as:

$$C_{sc}^{-2} = -\frac{2}{\epsilon\epsilon_0 e N_A A^2} (E - E_{FB} - kT), \tag{1}$$

where ϵ is the dielectric constant for Al oxide, ϵ_0 the permittivity of space $8.854 \times 10^{-14} \text{ F cm}^{-1}$, e the electron charge $1.602 \times 10^{-19} \text{ C}$, E the applied potential (V), E_{FB} the flat band potential (V), k the Boltzmann constant equal to $8.16 \times 10^{-5} \text{ eV/K}$, T the absolute temperature (K), A the sample area (cm^2) and N_A is the acceptor concentration (cm^{-3}).

Oxide formed on Al alloy shows the negative slope of the Mott-Schottky plot (Fig. 4), regardless of the presence or absence of mediator used during anodization, and regardless

¹ Data fitting was performed with Z View software package.

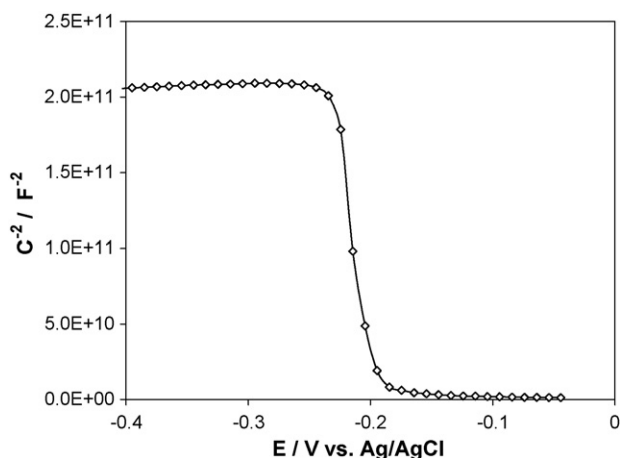


Fig. 4 – Typical Mott-Schottky plot of anodized Al alloy surface. Figure represents data for $E_{max} = 0.6 \text{ V}$, scan rate 50 mV/s , $[\text{Na}_2\text{SO}_4, 0.1 \text{ M}]$.

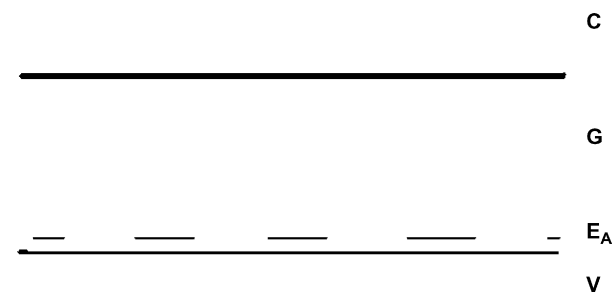


Fig. 5 – Zone diagram of aluminium oxide with the acceptor conductivity type.

of the chemical structure of mediator. This negative slope is characteristic for p type of conductivity (Fig. 5) that can occur, for example, due to a partial substitution of Al^{3+} ions by Si^{4+} ions, therefore creating a hole. Similar experiments on chemically pure Al result in different types of conductivity, depending on experimental conditions, similar to the phenomenon observed for nickel (Sikora and Macdonald, 2002).

Knowing the slope of MS plot around OCP, the acceptor concentration (N_A) can be calculated from Mott-Schottky relationship Eq. (1). Table 2 shows N_A for different compounds normalized to the highest value observed for CAT ($1.4 \times 10^{18} \text{ cm}^{-3}$). Different mediators used during the anodization produced different acceptor concentration (Table 2), possibly due to different valences of Al that could present in both hydrated and dehydrated forms. Substitution of Al^{3+} by Al^{2+} or Mg^{2+}

Table 2 – The relative acceptor concentration ($N_A/N_{A,max}$) obtained at 0.6 V in the presence of different mediators (normalized to the concentration at CAT)

Compounds	$N_A/N_{A,max}$
CAT	1
RES	0.602
HQ	0.679
HQS	0.270
BDS	0.292
DHBDS	0.138

Table 3 – Flat band potential of different compounds with only hydroxyl substitutions obtained at different E_{\max}

Compounds	Position of hydroxyl substitutions	E_{FB} (eV)		
		0.6 ^a	1.2 ^a	1.8 ^a
CAT	1, 2	-4.53	-4.60	-4.63
RES	1, 3	-4.60	-4.64	-4.64
HQ	1, 4	-4.63	-4.62	-4.61

^a E_{\max} (V) vs. Ag/AgCl.

liberates electron that recombine with a hole, therefore decreasing the carrier concentration.

Flat band potential was determined by converting the intersection of tangential to MS curve at OCP with abscissa to an energy scale in electron volts (Micaroni et al., 2000) by formula:

$$E_{\text{FB}} = -4.5 - E(\text{V/NHE}), \quad (2)$$

where E (V/NHE) is the potential versus normal hydrogen electrode (NHE) and E_{FB} is the flat band potential (eV).

The correlation between the position of hydroxyl substitutions and E_{FB} was found for the mediators with only hydroxyl substitutions in benzene ring (Table 3) for oxide formed at 0.6 V versus Ag/AgCl. Oxide formed in the presence of mediator with closer positions of hydroxyls possessed less electron affinity than the one formed in the presence of mediator with larger displacement of hydroxyl groups. Oxide formed at larger E_{\max} did not show this correlation.

The dependence of E_{FB} on the potential E_{\max} is shown in Table 3 and Fig. 6. E_{\max} governs the thickness of an oxide layer, and possibly E_{FB} barrier that electrons have to overcome to be removed from the oxide. E_{FB} is larger at higher E_{\max} . This principle was confirmed for CAT and somewhat for RES (Table 3); however it did not hold for HQ showing correlation with the proximity of hydroxyls in benzene ring on $E_{\text{FB}}-E_{\max}$ dependence. References for electrochemical oxidative polymerization of HQ (Levine et al., 2005b; Foos and Erker, 1986; Yamamoto et al., 1990) and CAT (Davis et al., 1997) can be found in literature. No literature data for electrochemi-

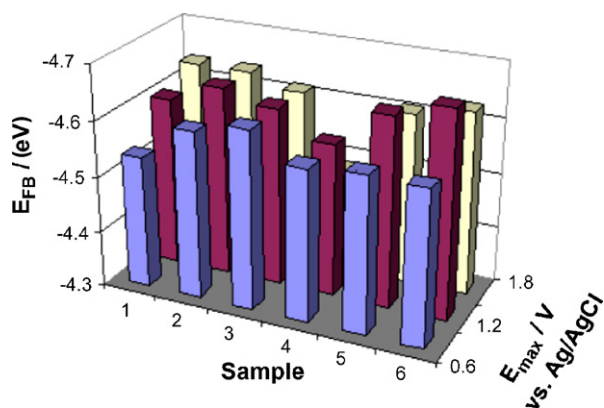


Fig. 6 – E_{FB} for different samples as a function of E_{\max} used for samples preparation. Numbers at “Sample” axes of the diagram state for the compound used for each set of tests: (1) CAT, (2) RES, (3) HQ, (4) HQS, (5) BDS and (6) DHBDS.

Table 4 – Flat band potential of different compounds with sulfonate substitutions obtained at different E_{\max}

Compounds	Sulfonate position	E_{FB} (eV)		
		0.6 ^a	1.2 ^a	1.8 ^a
HQS	1	-4.57	-4.57	-4.48
BDS	1, 3	-4.58	-4.64	-4.61
DHBDS	1, 3	-4.58	-4.67	-4.63

^a E_{\max} (V) vs. Ag/AgCl.

cal oxidative polymerization of RES was available. Continuous anodizing of a platinum panel in a solution containing RES monomer at positive 1 V for 1 h did not show any film formation, proving that RES does not polymerize at applied experimental conditions. CAT polymerization at Al surface was not observed in these experiments, traces of HQ polymerization were noticeable. Possibly, poly(HQ) affects E_{FB} at Al oxide surface, lowering E_{FB} at larger E_{\max} . Therefore, galvanic coupling between poly(HQ) and Al oxide is possible.

Summarizing, below positive 0.6 V (below CAT and HQ polymerization potential at Al), correlation between the position of hydroxyl group and E_{FB} , determined by MS analysis was observed. Above 1.2 V (above CAT and HQ polymerization potential on Al), correlation was not observed, because polymerization of a mediating compound was competing with the oxide formation. The case where RES was used as the mediator was an exception.

Table 4 summarizes E_{FB} for compounds with sulfonate substitutions. Mediators with sulfonate substitutions are known not to polymerize at experimental conditions applied. Anodizing at positive 0.6 V gives close E_{FB} values regardless of the amount of sulfonate substitutions and their position relatively to hydroxyl groups. Increased anodization potential results in increased E_{FB} with increased number of SO_3^- substitutions. In the experiments where compounds with two SO_3^- substitutions per single molecule were tested, E_{FB} was increasing with the increased number of hydroxyl substitutions (from the absence of hydroxyl substitutions in BDS to two substitutions in DHBDS), suggesting that both hydroxyl and sulfonate groups interact with aluminium oxide during its formation. Largest E_{FB} values were observed for DHBDS, reflecting the fact that electrons have to overcome the largest barrier to leave surface. The best corrosion protection performance of samples prepared with DHBDS was supported by laboratory monitoring.

5. Conclusions

Due to the complicated structure of Al alloy, the Al oxide formed on its surface contains impurities and deviations from stoichiometry. Si^{4+} substitutions create vacancies, while Al^{2+} or Mg^{2+} generate interlattice electrons. The concentration of these charge carriers defines the type and magnitude of the electrical conductivity of the oxide. Electron transfer mediators applied during the oxide deposition affect the balance between p and n defects in Al oxide that is a p type semiconductor in the case of Al alloy. Flat band potential and the

acceptor concentration were found to correlate with the structure of a mediator applied during the oxide deposition.

Acknowledgements

Authors would like to sincerely acknowledge Dr. Alda Simoens (Lisbon University of Technology, Portugal), and Dr. Valery Afanasiev (University of Leven, Belgium) for valuable discussions. Dr. Pete Peterson from Gamry Electrochemical Systems for his help with instrumentation. Help of corrosion team: Dr. Jie He, Mr. Dante Battocchi and Dr. Olga Stafford is sincerely appreciated.

This work was supported by the Air Force Office of Scientific Research (grant no. FA9559-04-1-0368) and also by the United States Air Force Research Laboratory, University of Dayton (grant no. RSC02050).

REFERENCES

- Bondarenko, A.S., Ragoisha, G.A., 2005. *J. Solid State Electrochem.* 9, 845–849.
- Davis, J., Vaughan, D.H., Cardosi, M.F., 1997. *Electrochim. Acta* 43 (3–4), 291–300.
- Foos, J.S., Erker, S.M., 1986. *J. Electrochem. Soc.* 133, 836.
- Iroh, J.O., 2001. *Surf. Eng.* 17, 265–267.
- Koch, G.H., 2002. Corrosion costs and preventive strategies in the United States. F.H.A. U.S. Dept. of Transportation, publication FHWA-RD-01-156.
- Levine, K.L., Tallman, D.E., Bierwagen, G.P., 2005a. *ECS Trans.* 1 (4), 81–91.
- Levine, K.L., Tallman, D.E., Bierwagen, G.P., 2005b. *Aust. J. Chem.* 58 (4), 294–301.
- Lorengel, M.M., 1993. *Mater. Sci. Eng. R11*, 243–294.
- Mathias, M.F., Haas, O., 1992. *J. Phys. Chem.* 96 (7), 3174–3182.
- Micaroni, L., Polo da Fonseca, C.N., Decker, F., De Paoli, M.-A., 2000. *Sol. Energy Mater. Sol. Cells* 60, 27–41.
- Mott, N.F., 1939. *Proc. Roy. Soc., A* 171, 27.
- Naoi, K., Takeda, M., Kanno, H., Sakakura, M., Shimada, A., 2000. *Electrochim. Acta* 45 (20), 3413–3421.
- Schottky, W.Z., 1939. *Physics* 113, 367.
- Sikora, E., Macdonald, D.D., 2002. *Electrochim. Acta* 48 (1), 69–77.
- Simons, W., Hubin, A., Vereecken, J., 1999. *Electrochim. Acta* 44, 4373–4381.
- Tallman, D.E., Vang, C., Wallace, G.G., Bierwagen, G.P., 2002. *J. Electrochem. Soc.* 149 (3), 173–179.
- Tolstopyatova, E.G., Sazonova, S.N., Malev, V.V., Kondratiev, V.V., 2005. *Electrochim. Acta* 50 (7–8), 1565.
- Yamamoto, K., Asada, T., Nishide, K., Bull, A.T., 1990. *Chem. Soc. Jpn.* 63, 1211.